Journal of
Materials Chemistry B

Accepted Manuscript

ROYAL SOCIETY OF CHEMISTRY

www.rsc.org/materialsB

Formulation of Robust Organic-Inorganic Hybrid Magnetic Microcapsules through Hard-Template Mediated Method for Efficient Enzyme Immobilization

Chen Hou, Yang Wang, Yanfeng Li*, Hao Zhu

State Key Laboratory of Applied Organic Chemistry, Key Laboratory of Nonferrous Metal Chemistry and Resources Utilization of Gansu Province, College of Chemistry and Chemical Engineering, Institute of Biochemical Engineering and Environmental Technology, Lanzhou University, Lanzhou 730000, China

A mild and facile method for the construction of robust organic-inorganic hybrid magnetic microcapsules was developed by a hard-template mediated method coordinated with polydopamine (PDA) and Fe_3O_4 nanoparticles onto $CaCO_3$ microparticle template. More specifically, negatively charged Fe_3O_4 nanoparticles were adsorbed on the surface or into the lumen of porous $CaCO_3$ microparticles through electrostatic interaction and physical absorption. Then the magnetic sacrificial templates were coated with PDA through self-polymerization of dopamine to obtain the magnetic PDA-$CaCO_3$ microparticles, which were followed by the template removal using EDTA to construct organic-inorganic hybrid magnetic microcapsules. Characterizations confirmed the microcapsules possess a robust hollow structure so that enzyme inside exists in a free state. The Fe_3O_4 nanoparticles acted critical factors in microcapsules for both recyclable component and tough scaffold to sustain the microcapsules away from collapse and fold. Combing the merits of the organic layer and inorganic component, the microcapsules were applied for encapsulation of

*Corresponding author. Tel: 86-931-8912113. E-mail address: liyf@lzu.edu.cn (Yanfeng Li)

Candida Rugosa Lipase (CRL). The encapsulated CRL was demonstrated to have several advantages, including increased encapsulation efficiency, enzyme activity and long-term storage stability. Hopefully, the as-prepared microbioreactor may provide a facile and generic approach for other biochemical applications.

1. Introduction

Protein capsules with tailored structures and properties have intrigued increased interesting from scientific research to technological applications such as drug/gene delivery, biocatalysis, bioreactor and nutrition[1-4]. When applied in specific applications, high reactive activity, controllable wall structure, and tunable protein loading amount of protein capsules should be possessed. More importantly, preferred materials to prepare protein capsules should be biocompatible, non-toxic, the operation conditions should be facile, moderate, and avoided use of harmful organic solvents and chemical cross-linkers.

The method currently used to fabricate protein capsules include sol-gel processing, emulsion/phase separation and layer-by-layer (LbL) self-assembly technique etc.[5], which proteins can be encapsulated either in the capsule lumen or within the multilayer shells in a controlled mode[6]. Yu et al. and Wang et al. prepared protein capsules by protein adsorption on mesoporous silica particles templates followed by LbL self-assembly of polyelectrolyte and template removal in hydrofluoric acid buffer[7, 8]. Chang et al. reported an easy one-pot microemulsion-templating method for protein encapsulation[9, 10]. Cui et al. prepared protein capsules by a one-step interfacial polymerization method and the emulsion template was removed by ethanol[11].

Although these methods demonstrated their success, some of them are inevitably suffered from tedious and time-consuming process as well as involving organic reagents and harsh post-treating conditions (such as heating, UV irradiation) which are environment unfriendly and protein deactivated[12, 13]. Besides, the expanded capsulizing procedures mainly composed of LbL technique which is charge-dependent interactions can be disintegrated by mutation of the pH value or the ionic strength of the surroundings, resulting in distortion, breakage, or even decomposition of capsules. Therefore, developing some facile and generic approaches for the preparation of protein capsules with desirable performance and ultimately scalable production are highly desired.

Our approach was inspired by the latent significance of organic-inorganic hybrid materials. Organic-inorganic hybrid materials such as carbon molecular sieves (CMS), metal-organic frameworks (MOFs), porous organic frameworks (POFs), have been widely used as outstanding templates and precursors to fabricate porous carbons and related functional materials based on their high surface areas, delicate structures, controllable features and abundant metal/organic species in their scaffolds[14-16]. Comprehensively, it would be ingenious and effectual to incorporate the superior separation performance and operational stability of inorganic component and the profound functionality and flexibility of organic material to fabricate hybrid microcapsules in a facile and controllable way.

In this study, we first introduced the magnetic property to construct the polydopamine (PDA) microcapsules to fabricate the well biocompatible and non-toxic

microenvironment for enzyme immobilization with convenient practical application helped by magnetic field. PDA as a wall component provides a simple, green and efficient approach to form a biocompatible microbioreactor with a thick-controllable, uniform and interconnectivity outer shell. In particular, the prepared magnetic PDA microcapsules not only showed practical application importance which can be easily recycled by an external magnetic field, but also helped to sustain the robust, plump, and spherical microcapsules structure when incorporated Fe_3O_4 nanoparticles in the inner wall of PDA layer. As for Enzyme immobilization, CRL was encapsulated in the microcapsules accompanied with $CaCO_3$ templates formation and then the CRL microcapsules were formed by template removal using EDTA. The shell thickness and the protein loading amount was tuned by the dopamine amount and protein doping amount, respectively. The activities and stabilities of the enzyme microcapsules over pH, temperature, kinetic behaviors, recyclability and storage time were investigated as well.

2. Experimental Section

2.1 Materials

$FeCl_3 \cdot 6H_2O$ and $FeCl_3 \cdot 6H_2O$ were purchased from AiHua Fine Chemicals Co., Ltd. (China); Dopamine hydrochloride, Candida rugosa lipase (CRL, Type VII) and Bovine serum albumin (BSA) were purchased from Sigma Chemical Co.; Tris(hydroxymethyl)-amiomethane (Tris), ethylenediamine tetraacetic acid disodium (EDTA), hydrochloric acid (HCl), and other chemicals and reagents were analytical grade, obtained from Tianjing Chemical Reagent Company (China).

2.2 Preparation of citric acid coated Fe_3O_4 nanoparticles

Citric acid coated Fe_3O_4 nanoparticles were prepared via co-precipitation of $FeCl_3 \cdot 6H_2O$ and $FeCl_3 \cdot 6H_2O$ by the addition of $NH_3 \cdot H_2O$[17]. In a typical procedure, 3.25 g $FeCl_3 \cdot 6H_2O$ and 1.195 g $FeCl_2 \cdot 4H_2O$ were completely dissolved in 50 ml deionized water in a 100 mL round-bottom flask. The aqueous solution was heated to 50 °C to obtain a clear yellow solution under vigorous stirring and purged with N_2. After 30 min, 6.25 ml $NH_3 \cdot H_2O$ was added into the round-bottom flask dropwise and the temperature was raised to 75 °C with the stirring continued for 60 minutes. After that, 1.5 M 6.25 ml trisodium citrate was introduced, the temperature was raised to 85 °C and the stirring continued for another 90 minutes under N_2. After the reaction completed, the black precipitate was collected by an external magnetic field, followed by washing several times with saturated sodium chloride, abundant deionized water and ethanol successively. Finally, the nanoparticles were dried at 40 °C in an oven under vacuum for 24 h.

2.3 Preparation of magnetic $CaCO_3$ microparticles

Uniform, spherical $CaCO_3$ microparticles with narrow size distribution (~3 μm in size) were prepared by colliodal crystallization from supersaturated solution[18]. Typically, 0.33 M Na_2CO_3 solution was rapidly poured into an equal volume of 0.33 M $CaCl_2$ solution at room temperature with intense agitation on a magnetic stirrer for 30 seconds, and after settling without stirring for 10 minutes, the white precipitate was filtered off, throughly washed with deionized water and ethanol, then dried in air.

To prepare magnetic $CaCO_3$ microparticles, 0.1% (w/v) Fe_3O_4 nanoparticles was

suspended in deionized water and stirred under ultrasonic for 20 minutes. Then $CaCO_3$ microparticles (10 mg ml^{-1}) were added to the above suspension and stirred mildly for another 30 minutes. After that, the black brown powder was collected by an external magnetic field, followed by washing several times with deionized water and ethanol, and dried at 40 °C in an oven under vacuum for 24 h.

2.4 Preparation of magnetic PDA microcapsules

100 mg Fe_3O_4 doped $CaCO_3$ microparticles was suspended in Tris-HCl buffer (40 ml, 50 Mm, pH 8.5) with a concentration of 2 mg ml^{-1}, 4 mg ml^{-1} and 8 mg ml^{-1} of dopamine hydrochloride. The polymerization was proceed for 10 h with constant stirring at ambient temperature. Next, the black microparticles were collected by an extenal magnetic field, and washed with fresh Tris-HCl buffer until the supernatant became colorless. The magnetic PDA microcapsules were obtained after removal of $CaCO_3$ microparticles with 0.1 M EDTA solution at room tempreture.

2.5 Assay of CRL immobilization

2.5.1 CRL immobilization

A certain amount of CRL was dissolved in 1 ml of Tris-HCl buffer solution (50 Mm, pH 7.0). The enzyme solution was added into 4 ml of 0.33 M $CaCl_2$ solution and the CRL doped magnetic PDA microcapsules were prepared following the same procedure described as above (section 2.3-2.4). After the reaction completed, the immobilized CRL was filtered off and washed with Tris-HCl buffer solution (50 Mm, pH 7.0) several times to remove the unreacted CRL. Especially, the reaction solution and washing solution were collected to assay the amount of residual lipase.

2.5.2 Determination of Immobilization Efficiency and Lipase Activity

The immobilization efficiency was expressed by the amounts of enzyme bounded on supports of unite mass, and the amount of enzyme was determined by the Bradford method[19], using BSA as the standard. The enzymatic activities of free and immobilized lipase were measured by the titration of the fatty acid which comes from the hydrolysis of olive oil[20] and reverse titration was adopted. One unit of lipase activity (U) is defined as the amount of enzyme needed to hydrolyze olive oil liberating 1.0 μmol of fatty acid per min in the assay condition.

The efficiency of immobilization was evaluated in terms of activity yields and immobilization yield as follows:

$$\text{activity yield (\%)} = \frac{C}{A}100\%$$

$$\text{immobilization yield (\%)} = \frac{A-B}{A}100\%$$

Where A is the activity of lipase added in the initial immobilization solution, B is the total activity of the residual lipase in the immobilization and washing solution after the immobilization procedure, and C is the activity of the immobilized lipase, respectively.

The relative activity (%) is the ratio between the activity of every sample and the maximum activity of the sample.

The residual activity (%) is the ratio between the activity of each sample and the initial activity of the sample.

All data used in these formulas are the average of triplicate of experiments.

2.5.3 Effect of pH and temperature of free and immobilized lipase activities

A certain amount free and the immobilized CRL were incubated in 0.1 M 50 ml phosphate buffer under the variety of pH (3.0-9.0) by hydrolysis of olive oil in a water bath at 37 °C for 30 min with continuous stirring, respectively. Then the enzymatic activities were determined and the relative activity was calculated.

The effect of temperature on the activities of free and the immobilized CRL were measured among the temperature range of 20-90 °C for 30 min and the relative activity was compared.

2.5.4 Reusability and storage stability

The reusability of immobilized CRL were determined by hydrolysis of olive oil with the recovered lipase after magnetic separation and thoroughly washed with phosphate buffer (0.1 M pH 7.0). Finally, the activities of the subsequent enzymatic reaction were compared with that of the first running (relative activity defined as 100%).

The storage stability was determined by measuring the residual activity of encapsulated CRL at 37 °C after it was stored at 4 °C for a certain period of time.

2.5.5 Kinetic Parameters (K_m and V_{max}) of free and immobilized CRL

The Michaelis constant (K_m) and the maximum reaction velocity (V_{max}) of free and immobilized CRL were determined by measuring initial rates of the reaction in phosphate buffer (0.1 M, pH 7.0) at 37 °C. Equivalent free or the immobilized CRL was added into olive oil emulsification solution with different concentrations from 0.4-2.0 mg ml^{-1}, and the enzymatic activities were determined. K_m and V_{max} for the free and immobilized CRL were calculated using the Michaelis-Menten model:

$$\frac{1}{V} = \frac{K_m}{V_{max}} \times \frac{1}{[S]} + \frac{1}{V_{max}}$$

where V (U mg^{-1}) was the initial reaction rate, [S] (ml mg^{-1}) was the initial substrate concentration, V_{max} (U mg^{-1}) was the maximum reaction rate obtained at infinite initial substrate concentration, and K_m (mg ml^{-1}) was the Michaelis-Menten contant.

2.6 Characterization

Fourier transform infrared (FTIR) spectra were obtained in transmission mode on a FTIR spectrometer (American Nicolet Corp. Model 170-SX) using the KBr pellet technique. The morphologies of the samples were characterized by a field-emission scanning electron microscopy (SEM, Hitachi S-4800, Japan) and transmission electron microscope (TEM, FEI Tecnal G^2F30) equipped with energy-dispersive X-ray spectroscopy (EDX, Oxford Instrument), high angle annular dark field (HAADF) and scanning transmission electron microscopy (STEM) to elucidate the dimensions and the structural details of the microcapsules. Magnetization measurements were performed on a Vibrating sample magnetometer (LAKESHORE-7304, USA) at room temperature. The thermal stability of samples was studied with a thermogravimetry (TG) analyzer (STA449C, Netzsch, Germany) at heating rate of 10 °C min^{-1} in a nitrogen atmosphere.

3. Result and discussion

3.1 Preparation and characterization of hybrid microcapsules

Our approach to formulate hybrid microcapsules by depositing polydopamine onto magnetic sacrificial template is shown in Fig. 1. Construction of biological capsules is limited by the crucial prerequisite conditions such as mild formation and gentle

removal of tempaltes. The porous $CaCO_3$ microparticles have been widely used as templates for bioactive compounds encapsulation[14, 21-23]. The pore size distribution of the as-prepared $CaCO_3$ microparticles is from 20 to 60 nm and the ξ-potential at pH 7.0 is positively charged[18]. Based on the ingenious features, $CaCO_3$ microparticles can adsorb negatively charged Fe_3O_4 nanoparticles (modified by citric acid in this work) with a diamer of about 10-15 nm into the lumen or on the surface of $CaCO_3$ microparticles. After the spontaneous self-polymerization of dopamine on the surface of the magnetic $CaCO_3$ template, the subsequent dissolution of $CaCO_3$ using EDTA was performed so that the complex of Ca^{2+} with EDTA could easily permeate through the polymer walls. Thus the PDA-Fe_3O_4 microcapsules were successfully acquired.

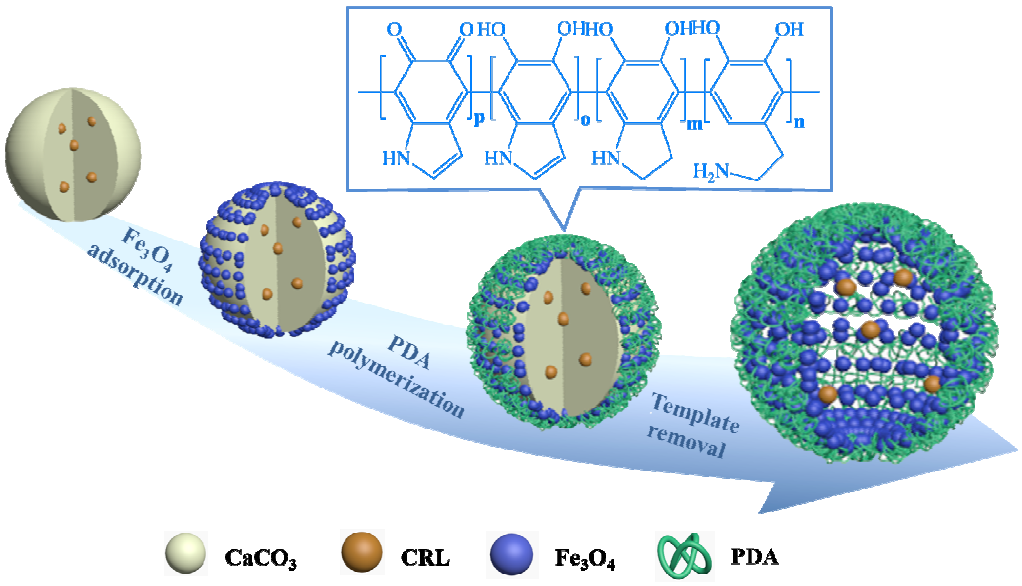

Fig. 1 Schematic illustration of the synthesis process used to produce Fe_3O_4-PDA microcapsule.

The morphologies of the prepared magnetic $CaCO_3$ templates are characterized by SEM and TEM. As shown in Fig. 2, the spherical $CaCO_3$ microparticles with a diameter about ~3 μm possessed porous, channel-like internal structure (Fig. 2a, b).

Actually, the microparticles were fromed by the instant aggregation of amorphous nanoprecipitates upon mixing the $CaCl_2$ and Na_2CO_3 solutions, and the size distribution and pore density of the $CaCO_3$ microparticles are directly dependent on the agitation speed. The rapid and intense agitation would lead to a smaller particle size and loose porous structure[23]. After adsorption of negatively charged Fe_3O_4 nanoparticles at neutral condition, the surface of $CaCO_3$ microparticles became coarse and texture overload (Fig. 2c, d), and it also can be observed clearly from the TEM images of magnetic $CaCO_3$ microparticles that many Fe_3O_4 nanoparticles were assembled on $CaCO_3$ microparticles (Fig. 2e, f), suggesting that the Fe_3O_4 nanoparticles were deposited homogeneously.

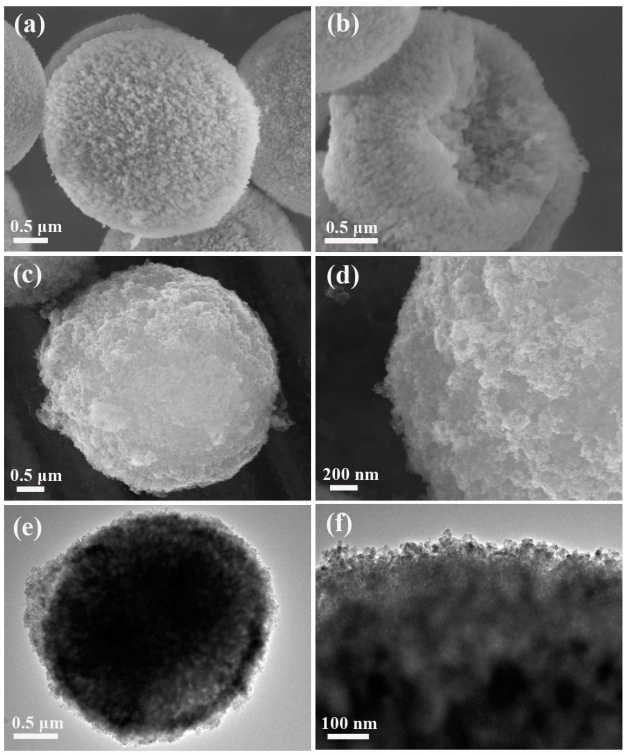

Fig. 2 SEM images of (a, b) $CaCO_3$ microparticles, (c, d) Fe_3O_4-$CaCO_3$ microparticles, and TEM images of (e, f) Fe_3O_4-$CaCO_3$ microparticles.

Several batches of Fe_3O_4-PDA microcapsules were prepared to vary the concentration of dopamine in reaction mixtures as followed: 2 mg ml^{-1} (PDA_2-Fe_3O_4), 4 mg ml^{-1} (PDA_4-Fe_3O_4), and 8 mg ml^{-1} (PDA_8-Fe_3O_4). As shown by SEM (Fig. 3), after PDA polymerization, the surface of the Fe_3O_4-$CaCO_3$ microparticles became rough with the increased concentration of dopamine (Fig. 3a, d, g), and high concentration of dopamine lead to a grainy surface, as illustrated in the case of PDA_8-Fe_3O_4-$CaCO_3$ microparticles (Fig. 3g). Interestingly, after template dissovled by EDTA, all the three kinds the PDA-Fe_3O_4 microcapsules holded the plump, spherical structure away from collapse and fold upon a large cavity (Fig. 3b, c, e, f, h, i), which is superior to the same sort of polymer microcapsules prepared in other reports[1,5,11,23,24]. This phenomenon can be attributed to the Fe_3O_4 nanoparticles wrapped in the thick PDA layers which acted as scaffold in each microcapsules.

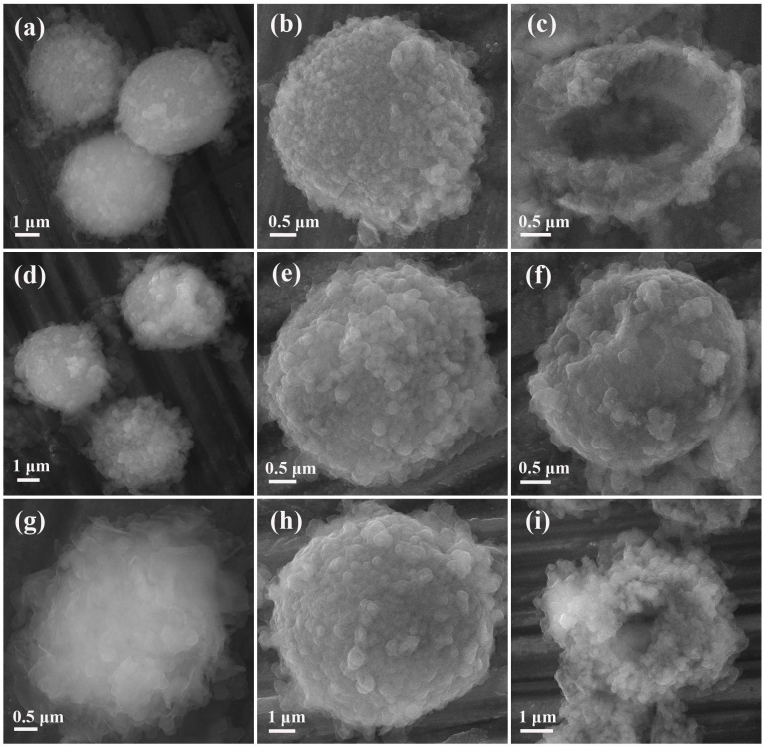

Fig. 3 SEM images of (a) PDA_2-Fe_3O_4-$CaCO_3$ microparticles, (b, c) PDA_2-Fe_3O_4 microcapsule, (d) PDA_4-Fe_3O_4-$CaCO_3$ microparticles, (e, f) PDA_4-Fe_3O_4 microcapsule, (g) PDA_8-Fe_3O_4-$CaCO_3$ microparticle, and (h, i) PDA_8-Fe_3O_4 microcapsule (half-capsules of c and i were made from broken $CaCO_3$ microparticles by grinding and ultrasound of the as-prepared $CaCO_3$ microparticles).

To further confirm the inner structure of PDA-Fe_3O_4 microcapsules, we conducted the TEM images. As can be seen from Fig. 4, after template removal the hollowed microcapsules were formed and no folds and creases appeared (Fig. 4 a, b, d, e, g, h). The wall of the microcapsules PDA_2-Fe_3O_4, PDA_4-Fe_3O_4, and PDA_8-Fe_3O_4 became thicker with the increase of the dopamine concentrations (Fig. 4 b, e, h). Besides, it can be clearly observed that Fe_3O_4 nanoparticles were wrapped in the polymer layer after $CaCO_3$ microparticles dissolution (Fig. 4 c, f, i). Thus, the hollow and intact structure of PDA-Fe_3O_4 microcapsules inheriting the superior structural stability of the hybid microcapsules were successfully obtained.

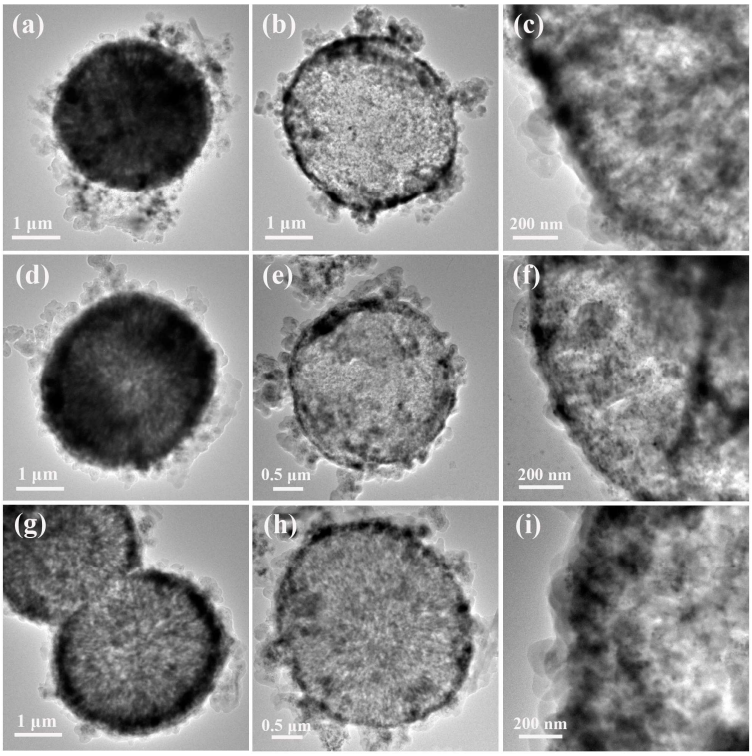

Fig. 4 TEM images of (a) PDA_2-Fe_3O_4-$CaCO_3$ microparticle, (b, c) PDA_2-Fe_3O_4 microcapsule, (d) PDA_4-Fe_3O_4-$CaCO_3$ microparticle, (e, f) PDA_4-Fe_3O_4 microcapsule, (g) PDA_8-Fe_3O_4-$CaCO_3$ microparticles, and (h, i) PDA_8-Fe_3O_4 microcapsule.

The functional groups of the as-prepared hybid microparticles and microcapsules were examined using FTIR (Fig. 5). Compared with pure $CaCO_3$ microparticles, new characteristic peak at 580 cm^{-1} of Fe_3O_4-$CaCO_3$ microparticles appeared after adsorption of Fe_3O_4 nanoparticles, which can be ascribed to the lattice absorption of Fe_3O_4 nanoparticles. In the spectrum of PDA_8-Fe_3O_4 microcapsules, the broad adsorption bands within new peaks at 1599 cm^{-1} and 1508 cm^{-1} originated from the benzene ring structure. The adsorption bands from 1400 to 1100 cm^{-1} can be attributed to $–CH_2$ bending vibration (1347 cm^{-1}), C-O-H asymmetric bending vibration (1288 cm^{-1}), C-O asymmetric vibration (1249 cm^{-1}) and C-N stretching vibration (1155

cm^{-1}), respectively[25]. In addition, it could be noted that the peak at about 3390 cm^{-1} of PDA_8-Fe_3O_4 microcapsules is broader than that of Fe_3O_4-$CaCO_3$ microparticles, which resulted from the overlapping of hydroxyls, water adsorbed in PDA polymer and amines of PDA[26].

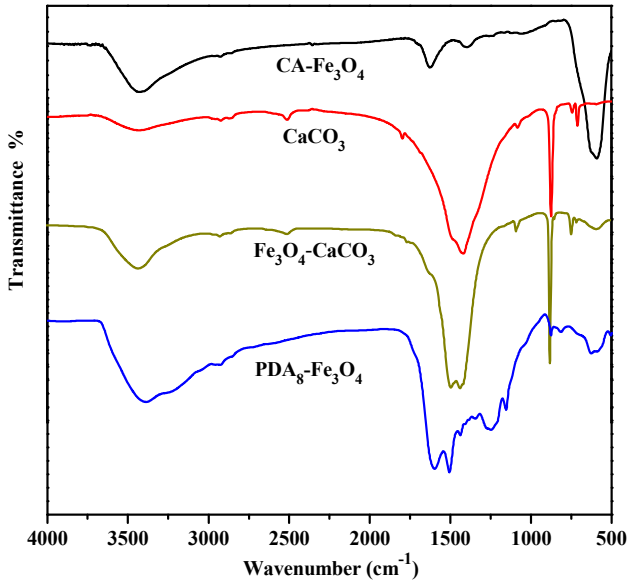

Fig. 5 FTIR spectra of the as-prepared CA-Fe_3O_4 nanoparticles, $CaCO_3$ microparticles, Fe_3O_4-$CaCO_3$ microparticles, and PDA_8-Fe_3O_4 microcapsules.

The composition of PDA-Fe_3O_4 microcapsules were characterized by TG analysis under N_2 atmosphere (Fig. 6). CA-Fe_3O_4 showed a mild weight loss (3.7 wt%) below 200 °C which can be assigned to the evaporation of absorbed water and solvent. When the temperature rose to 400 °C, another weight loss (2.3 wt%) was observed due to the decomposition of citric acid. Then it kept no decline until the temperature rose to 800 °C which is indicative of the remarkable thermo-stability of Fe_3O_4. The TG curves of three kinds of PDA-Fe_3O_4 microcapsules retained the same trend under 200 °C until the temperature rose to 600 °C. A large mass loss (43.7 wt% for PDA_2-Fe_3O_4, 45.1 wt% for PDA_4-Fe_3O_4, and 48.8 wt% for PDA_8-Fe_3O_4, respectively)

was observed between 200 and 700 °C which was resulted from the decomposition of PDA. TG analysis also improved the successful preparation of the magnetic hybrid microcapsules.

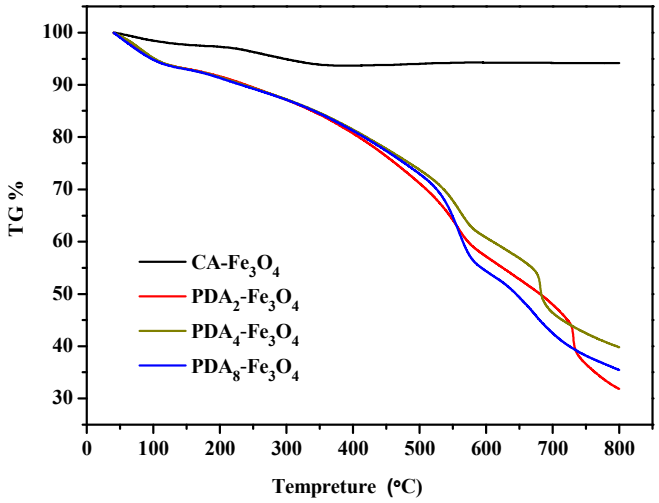

Fig. 6 TG curves of CA-Fe_3O_4 nanoparticles and PDA-Fe_3O_4 microcapsules.

Next, energy-dispersive X-ray spectroscopy elemental mapping was used to understand the distribution of elements in the microcapsules. From the elemental distribution of carbon, nitrogen, oxygen and iron in Fig. 7, we can recognize that C, N, O and Fe distributed uniformly throughout the specific area in PDA_8-Fe_3O_4 microcapsules. To further characterize the porosity of PDA_8-Fe_3O_4 microcapsules, BET analysis was employed. The specific surface area of hybrid layer was 29 m^2 g^{-1}, the pore size and volume were 15.6 nm and 0.11 m^3 g^{-1}, respectively. Thus, the mesoporous structure of the hybrid microcapsules would act as a semipermeable membrane which could selective through molecules to prevent the large encapsulated molecules (cell and proteins) from leaching and make small molecules access and leave easily[22].

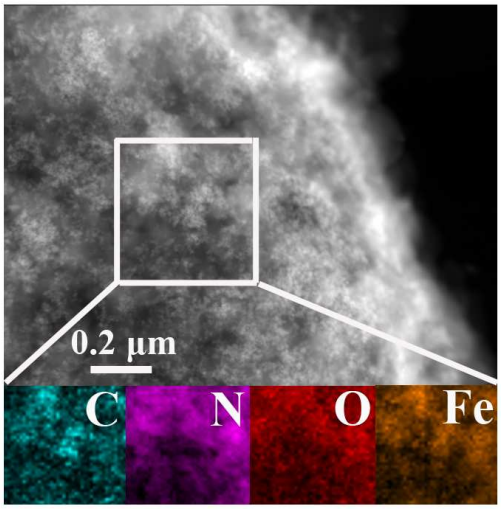

Fig. 7 STEM image and corresponding carbon, nitrogen, oxygen and iron elemental mapping of PDA_8-Fe_3O_4 microcapsules.

The hysteresis loops of the prepared magnetic nanoparticles are shown in Fig. 8. From Fig. 8 we can see that the saturation magnetization (MS) values are about 59.21 emu g^{-1} for CA-Fe_3O_4 nanoparticles, 19.45 emu g^{-1} for Fe_3O_4-$CaCO_3$ microparticles and 21.72 emu g^{-1} for PDA_8-Fe_3O_4 microcapsules, respectively. Although the MS value of PDA_8-Fe_3O_4 microcapsules declined seriously, it still has an accepted property for simple magnetic separation. Furthermore, there are no hysteresis in the magnetization with both remanence and coercivity being zero, indicating that the as-prepared PDA_8-Fe_3O_4 microcapsules are superparamagnetic at room pempreture[27]. The insert of Fig. 8 demonstrated that PDA_8-Fe_3O_8 microcapsules can be easily manipulated by an external magnetic field, which reveals that the magnetic support possessed a suitble property for magnetic actuation and manipulation.

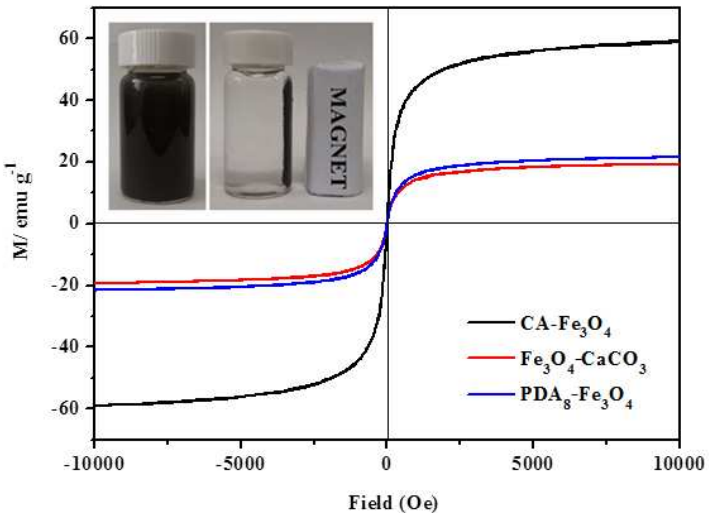

Fig. 8 Magnetic hysteresis loops of CA-Fe_3O_4 nanoparticles, Fe_3O_4-$CaCO_3$ microparticles, and PDA_8-Fe_3O_4 microcapsules (the insert is the schematic of the simple magnetic separation of PDA_8-Fe_3O_4 microcapsules).

3.2 Application of Fe_3O_4-PDA hybrid microcapsules for enzyme immobilization and enzyme catalysis

For the CRL immobilization, PDA_8-Fe_3O_4 microcapsules were used. The enzyme encapsulation efficiency for PDA_8-Fe_3O_4 microcapsules was investigated in detail. Specifically, the enzyme encapsulation efficiency was detemined with the enzyme concentration varied from 0.1 to 2.0 mg ml^{-1}. Accordingly, as shown in Fig. 9, the enzyme encapsulation efficiency decreased monotonically with the increase of enzyme concentration and the immobilized enzyme exhibited an increased activity, simultaneously. At the concentration of 1.0 mg ml^{-1}, the relative activity of immobilized CRL reached the highest value. Then it can be speculated that the CRL was easily to be entrapped by the $CaCO_3$ microparticles, which finally rendered enhanced effective enzyme encapsulation efficiency. Moreover, to evaluate the

enzymatic properites, the kinetics of the immobilized CRL with the concentration of 1.0 mg ml^{-1} in PDA_8-Fe_3O_4 microcapsules ($CRL_{1.0}$-PDA_8-Fe_3O_4) were calculated from an enzymatic assay by Michaelis-Menten enzyme kinetics model (Table 1). Compared with free CRL, the K_m for the $CRL_{1.0}$-PDA_8-Fe_3O_4 is lower than the free form, suggesting a higher affinity of the CRL towards the substrates after encapulation. The improved affinity was mainly due to the well biocompatibility of the PDA which provided increased access probability of the substrate molecules to contanct CRL in the appropriate inner microenviroment. V_{max} of the immobilized CRL is also lower than the free CRL, indicated that the microencapsulation restricted the activity of enzyme, which possibly due to the diffusional resisitance of the capsule wall.

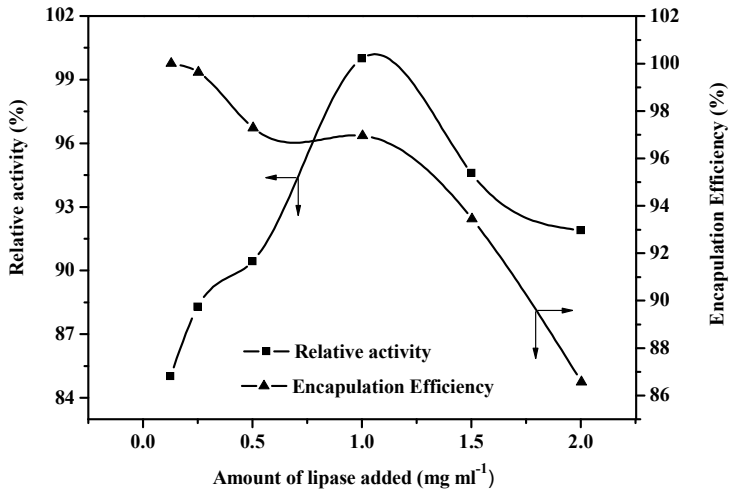

Fig. 9 Effect of enzyme amount and encapulation efficiency of PDA_8-Fe_3O_4 microcapsules.

Table 1. Kinetic Parameters of Free CRL and $CRL_{1.0}$-PDA_8-Fe_3O_4 microcapsules.

	K_m (mg ml^{-1})	V_{max} (U mg^{-1})

Free CRL	0.43	6.05
$CRL_{1.0}$-Fe_3O_4-PDA_8	0.32	5.04

The pH stability of $CRL_{1.0}$-PDA_8-Fe_3O_4 microcapsules and free CRL is compared in Fig. 10a. At pH 3.0, the free CRL retained 29% of the relative activity while $CRL_{1.0}$-Fe_3O_4-PDA_8 kept it at 59%. At pH 9.0, the free CRL retained 42% of the relative activity while $CRL_{1.0}$-PDA_8-Fe_3O_4 kept 89% of its initial activity. In addition, $CRL_{1.0}$-PDA_8-Fe_3O_4 showed broader pH scope. This phenomenon can be explained by the buffering effect of the organic layer of the microcapsules. The abundant –OH/-O^- pairs and the –NH_2/-NH_3^+ pairs on PDA made it a zwitter-ion under different pH range[28] which could tune the local pH value. Thus the CRL near the hybrid walls would stay in the buffer region against the environmental mutation.

When the hydrolysis for olive oil emulsion was operated at a series of temperature range, the immobilized CRL showed enhanced relative activities than the free CRL (Fig. 10b). Compared with free lipase, the immobilized CRL kept its relative activity up to 80% in the temperature range of 20-60 °C and exhibited mare than 60% of relative activity at 90 °C, revealed much superber heat endurance than that of the free lipase. It seemed that the robust hybrid wall structure conducted a tough performance with enzymes from denaturation at high temperatures.

The well reusability of lipase is critical for the potential application in industry. As presented in Fig. 10c, the immobilized enzyme kept the high activity at 75% after 12 times reuse due to the sturdy stability of the hybrid microcapsules which effectively ameliorated the denaturation and leakage of enzyme under multiple reaction circles.

The storage stability of $CRL_{1.0}$-PDA_8-Fe_3O_4 is shown in Fig. 10d. After storage at 4 °C for 35 days, $CRL_{1.0}$-PDA_8-Fe_3O_4 can matain the residual activity as high as 82%. The activity of the immobilized enzyme was significantly improved with a lowered decreasing rate. The enhancement of the stability revealed that the hybrid microcapsules could provide a feasible enviroment for the enzyme molecules based on the well biocompatible property of PDA layer and the integrated and tough wall structure of the hybrid microcapsules.

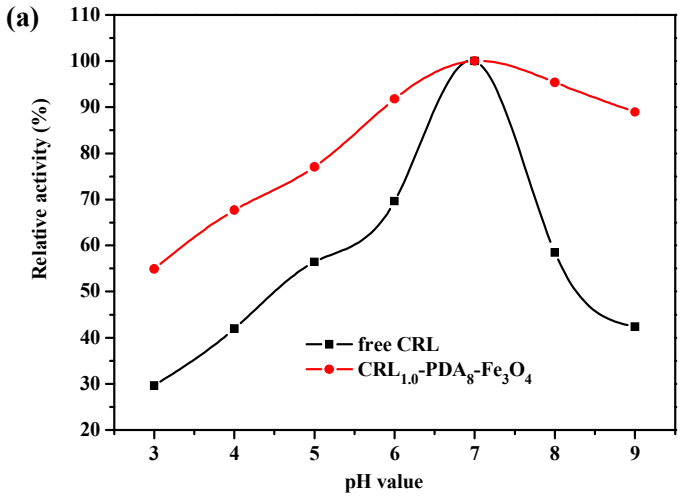

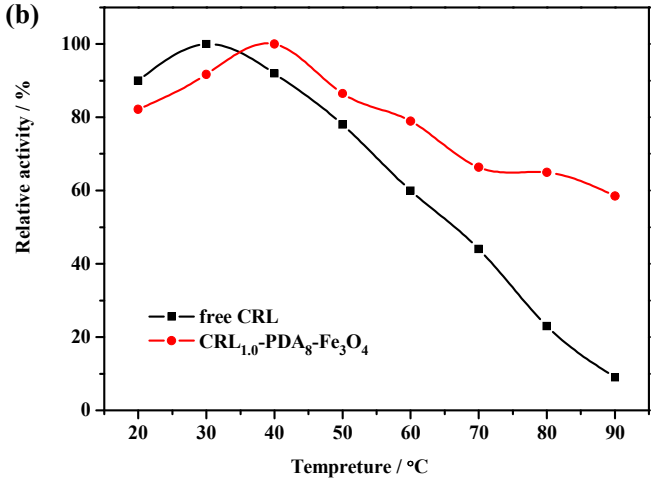

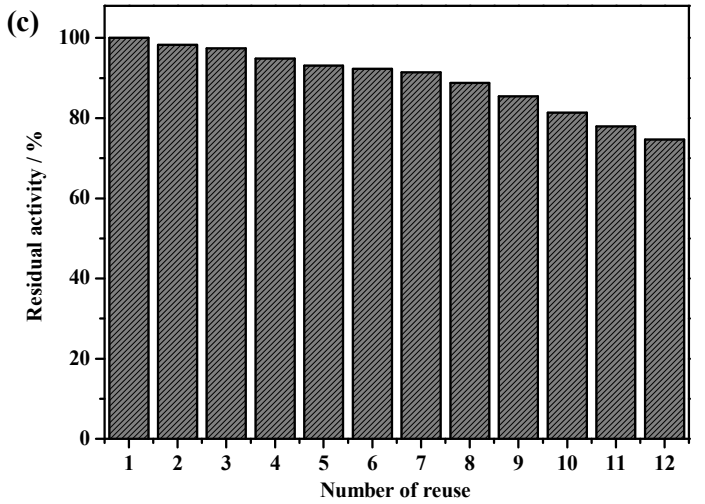

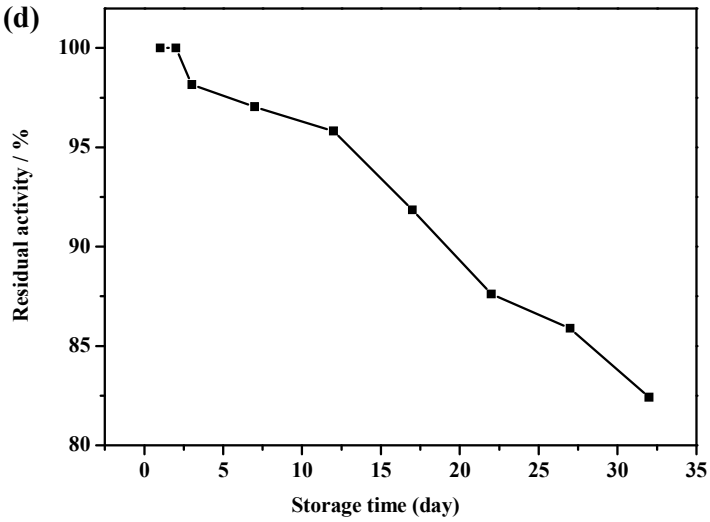

Fig. 10 Effect of (a) pH value, (b) temperature, (c) number of reuse, and (d) storage time of free and immobilized CRL.

4. Conclusion

We developed an easy and effectual method for the fabrication of robust organic-inorganic hybrid magnetic microcapsules by polydopamine coated magnetic porous $CaCO_3$ microparticle template. The Fe_3O_4 nanoparticles acted practical dual role in the formation of microcapsules; as the recyclable component in the hybrid microcapsules and the robust scaffold to sustain the microcapsules away from

collapse and fold or even rupture during the multiple-use. The shell thickness of the microcapsules could be easily controlled by the concentration of dopamine. Moreover, the as-prepared microcapsules exhibited excellent immobilization efficiency towards CRL. The well biocompatibility and non-toxicity of the hybrid microcapsules constructed a suitable microenviroment for the immobilized enzyme; especially the inorganic factor improved the rigidity of the wall to maintain the activity of the enzyme inside. The immobilized CRL demonstrated significant high mechanical stability and activity under various conditions, such as pH, temperature, reusability and storage time. It is reasonable to believe that the robust and flexible Fe_3O_4 doped PDA hybrid microcapsules are useful to be applied in many other fields both in material science and bio-applications.

Acknowledgements

The authors thank the financial supports from the National Natural Science Foundation of China (No.21374045), the scientific research ability training of under-graduate students majoring in chemistry by the two patters based on the tutorial system and top students (J1103307) and the Opening Foundation of State Key Laboratory of Applied Organic Chemistry (SKLAOC-2009-35).

References

1 X. L. Wang, J. F. Shi , Z. Y. Jiang, Z. Li, W. Y. Zhang, X. K. Song, Q. H. Ai and H. Wu, *Biomacromolecules*, 2013, 14, 3861-3869.

2 M. Morikawa, A. Takano, S. C. Tao and Nobuo Kimizuka, *Biomacromolecules*, 2012, **13**, 4075-4080.

3 K. K. Islets, S. Jhunjhunwala, J. Wu, A. Swanson, D. Gao and S. R. Little, *Angew. Chem., Int. Ed*., 2011, **50**, 8706-8708.

4 G. B. Sukhorukov, A. L. Rogach, B. Zebli, T. Liedl, A. G. Skirtach, K. Kohler, A. A. Antipov, N. Gaponik, A. S. Susha, M. Winterhalter and W. J. Parak, *Small*, 2005, **1**, 194-200.

5 F. Wang, J. Feng, W. J. Tong and C. Y. Gao, *J. Mater. Chem.*, 2007, **17**, 670-676.

6 R. C. Luo, S. S. Venkatraman and B. Neu, *Biomacromolecules*, 2013, **14**, 2262-2271.

7 A. Yu, Y. Wang, E. Barlow and F. Caruso, *Adv. Mater.*, 2005, **17**, 1737-1741.

8 Y. J. Wang and F. Caruso, *Chem. Mater.*, 2005, **17**, 953-961

9 F. P. Chang , Y. Hung , J. H. Chang, C. H. Lin and C. Y. Mou, *ACS Appl. Mater. Interfaces*, 2014, **6**, 6883-6890.

10 F. P. Chang, Y. P. Chen and C. Y. Mou, *Small*, 2014, **10**, 4785-4795.

11 J. Cui, Y. J. Wang, A. Postma, J. C. Hao, L. H. R and F. Caruso, *Adv. Funct. Mater.*, 2010, **20,** 1625-1631.

12 X. Y. Zhu, S. F. Guo, D. Janczewski, F. J. P. Velandia, S. L.-M. Teo and G. J. Vancso, *ACS Appl. Mater. Interfaces,* 2013, **5,** 5961-5968.

13 Q. Y. Yi, D. S. Wen and G. B. Sukhorukov, *Langmuir*, 2012, **28,** 10822-10829.

14 X. L. Wang , Z. G. Jiang , J. F. Shi , Y. P. Liang , C. H. Zhang and H. Wu, *ACS Appl. Mater. Interfaces*, 2012, **4,** 3476-3483.

15 J. K. Sun and Q. Xu, *Energy Environ. Sci.*, 2014, **7**, 2071-2100. **7**

16 H. V. Thang and S. Kaliaguine, *Chem. Rev.*, 2013, **113,** 4980-5028.

17 A. Goodarzi, Y. Sahoo, M. T. Swihart and P. N. Prasad, *Mat. Res. Soc. Symp. Proc.*, 2004, **789,** 6.6.1-6.6.6.

18 D. V. Volodkin, N. I. Larionova and G. B. Sukhorukov, *Biomacromolecules*, 2004, **5,** 1962-1972.

19 M. M. Bradford, *Anal. Biochem.*, 1976, **72**, 248-254.

20 Y. Omprakash and I. Toyoko, *Biomacromolecules*, 2005, **6**, 2809-2814.

21 J. Li, Z. G. Jiang, H. Wu, L. Zhang, L. H. Longa and Y. J. Jiang, *Soft Matter*, 2010, **6,** 542-555.

22 C. Y. Tian, C. H. Zhang, H. Wu, Y. X. Song, J. G. Shi, X. L. Wang, X. K. Song, C. Yang and Z. G. Jiang, *J. Mater. Chem. B*, 2014, **2,** 4346-4355.

23 G. B. Sukhorukov, D. V. Volodkin, A. M. Günther, A. I. Petrov, D. B. Shenoya and H. Möhwald, *J. Mater. Chem.*, 2004, **14**, 2703-2081.

24 J. F. Shi, C. Yang, S. H. Zhang, X. L. Wang, Z. Y. Jiang, W. Y. Zhang, X. K. Song, Q. H. Ai and C. Y. Tian, *ACS Appl. Mater. Interfaces*, 2013, **5**, 9991-9997.

25 M. Zhao, C. H. Deng and X. M. Zhang, *ACS Appl. Mater. Interfaces*, 2013, **5**, 13104-13112.

26 Y. X. Wang, S. H. Wang, H. Y. Niu, Y. R. Ma, T. Zeng, Y. Q. Cai and Z. F. Meng, *J. Chromatogr. A*, 2013, **1283**, 20-26.

27 K. E. Mooney, J. A. Nelson and M. Wagner, *Chem. Mater.*, 2004, **16**, 3155-3161.

28 B. Yu, J. X. Liu, S. J. Liu and F. Zhou, *Chem. Commun.*, 2010, **46**, 5900-5902.

Graphical abstract:

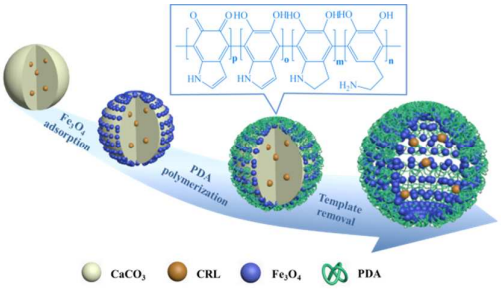

Fabrication of robust organic-inorganic hybrid magnetic microcapsules coordinated with polydopamine and Fe_3O_4 nanoparticles for enzyme immobilization.